Published in final edited form as:
Anal Biochem. 2007 April 1; 363(1): 35–45. doi:10.1016/j.ab.2006.12.029.

Immobilized Molecular Beacons: A New Strategy using UV-Activated PMMA Surfaces to Provide Large Fluorescence Sensitivities for Reporting on Molecular Association Events

Catherine Situma[1,2], **Amanda J. Moehring**[3], **Mohamed A. F. Noor**[3], and **Steven A. Soper**[1,2]

[1]Louisiana State University, Department of Chemistry Baton Rouge, Louisiana 70803

[2]Center for Bio-Modular Multi-Scale Systems, Baton Rouge, Louisiana 70803

[3]Department of Biology, Duke University, Durham, North Carolina 27708

Abstract

We have designed appropriately prepared solid supports consisting of poly (methyl methacrylate), PMMA, that provide enhanced performance levels for molecular beacons (MBs) that are used for recognizing and reporting on signature DNA sequences in solution. The attachment of primary amine-containing MBs to the PMMA surface was carried out by UV activating the PMMA to produce surface-confined carboxylate groups, which could then be readily coupled to the MBs using EDC chemistry. The fluorescence properties of the MBs covalently attached onto this UV-activated PMMA surface was evaluated and compared to the same MBs immobilized onto glass supports. We observed improved limits of detection for the solution complement to the MBs when immobilized onto PMMA, which was attributed to both the lower autofluorescence levels exhibited by PMMA at the detection wavelengths used and the improved quenching efficiency of the MBs when in their closed hairpin configuration when strapped to a PMMA surface as opposed to glass. As an example of the utility of the PMMA-based immobilization strategies developed for MBs, we report on the analysis of cDNAs specific for *fruitless* (*fru*) and *Ods-site homeobox* (*OdsH*) genes extracted from *Drosophila melanogaster* fruitflies. The *fru* gene functions in the central nervous system, where it is necessary for sex determination and male courtship behavior, while the *OdsH* gene is involved in the regulation of transcription.

Introduction

DNA/RNA detection probes that not only provide molecular recognition of unique structures, but also report on the molecular association through a fluorescence transduction event have become very attractive assemblies in a variety of applications. An example of such probes are molecular beacons (MBs) [1], which are hairpin probes consisting of a loop and stem structure. The loop portion is the sequence recognition section of the MB while the stem, which is comprised of complementary sequences, intra-molecularly hybridizes in the absence of the loop complement. On one end of the stem is a fluorophore, while the other stem possesses a quencher. Upon hybridization of the stems, the closed hairpin structure forms, placing in close proximity the fluorophore and quencher producing quenching of the fluorescence reporter either through contact mediation or energy transfer. When the recognition loop hybridizes to

its complementary target sequence, the stem opens restoring the fluorescence. These probes have found numerous applications, such as the detection of pathogenic retroviruses [2], discrimination of wild type and single point mutations [3;4], real time monitoring of DNA/RNA in solution/living specimens [1;5] and single nucleotide polymorphism detection [6].

While extensive research involving MB probes has been performed in homogeneous phases, surface immobilization of MBs has not been reported extensively. Surface immobilization has the advantage of allowing spatially multiplexed detection with a probe that not only offers selective affinity for its complement, but also reports on the molecular association obviating the need for labeling of the solution complement. The implementation of surface immobilized MBs or other molecular probes configured into an array format also enables the seamless integration of this technology to various sample processing steps by the direct coupling of the array to a microfluidic system, which offers high levels of automation and reduced sample and reagent consumption, lowering assay costs [7]. An additional advantage of MBs compared to their linear nucleic acid probes is their recognition specificity. By analyzing free energy phase diagrams of MBs in solution with matched and mismatched targets, structurally constrained MBs have been shown to distinguish mismatches over a wider range of temperatures than unstructured (linear) probes [8;9].

Unfortunately when MB probes are immobilized onto solid supports, they display lower sensitivities, where the sensitivity here is defined as the ratio of fluorescence of the probe upon binding to its target with that of the probe in its closed (non-fluorescent) form, compared to their solution-based counterparts. The lower sensitivity is due in part to inefficient quenching of the surface-attached MBs, which is caused by increased non-specific surface interactions with the solid support that destabilizes the hairpin structure. As such, a significant effort has been exploited into exploring various solid supports and appropriate probe designs that provide better sensitivities for MBs. For example, MBs have been attached onto optical fiber core surfaces via biotin-avidin/streptavidin interactions [10;11;12;13]; however, higher background noise from both the closed form (quenched) of the MB and the cladding of the optical fibers was an issue in these reports.

Glass has been widely used as a solid support for the immobilization of MBs [10;14;15;16]. Unfortunately, glass suffers from well-documented problems due primarily to interfacial effects; the static charging experienced by glass surfaces can partially open the closed hairpin structure resulting in high levels of fluorescence for the immobilized MB in its closed conformation. MBs have also been immobilized onto micro-wells/porous surfaces using agarose or polyacrylamide gel films, which provide a solution-like environment rather than the typical heterogeneous liquid-solid interface [17;18]. However, the use of these gel films slows the hybridization process due to diffusion-limited mass transport of the targets through the gel network.

Gold metallic surfaces have also been studied as viable substrates for the attachment of MB probes, where the gold serves the purpose of being a solid support and also, a quencher of the fluorescence [19;20;21;22]. Even though the MBs can be tethered easily onto gold surfaces via self-assembly of alkane thiols, nitrogen-based moieties along the probe's DNA backbone can chemisorb to these same surfaces resulting in non-specific adhesion of the DNA to the gold surface. Non-specific interactions of the solution target with the gold surface must be minimized by employing blocking agents to prevent the nitrogen containing nucleotide bases from interacting directly with the gold surface [20]. Other artifacts that that affect the sensitivity, specificity and hybridization kinetics of the MBs on gold include the non-uniform distribution of hairpin probes on the gold surface causing surface-induced aggregation [20; 23;24].

In another attempt to improve the sensitivity of surface-immobilized MBs, Zuo et. al. have designed MBs that contained a linker arm serving as a spacer and also a restriction site within the loop structure [25]. These authors reported improvements in the fluorescence sensitivity of 5.2-fold compared to glass and a MB not containing a restriction site. Their results also showed that the loop of the immobilized MB didn't open effectively upon hybridization with cDNA targets.

The reaction thermodynamics and kinetics of surface immobilized MBs differ from those in solution as a result of interfacial concentration gradients, species-interface interactions and steric hindrance. For example, surface electrostatics greatly affects the binding parameters of surface immobilized probes because of the wide distribution of probe-surface distances among these probes due to entropic effects, which can contribute to variations in hybridization melting temperatures [26;27;28]. For surface hybridization, nucleic acid targets can be repelled or attracted to the surface depending on the immobilization material as well. Electrostatic repulsion between single stranded nucleic acid targets and the surface immobilized probes (due to the high negative charge of nucleic acid oligomers) can result in Coulomb blocking of hybridization events. Tethered probes with long linker molecules have electrostatic interactions that can dominate short-range Van der Waals forces. Also, steric hindrance, which increases with increasing surface probe densities, can alter the hybridization efficiencies of surface immobilized probes due to the presence of repulsive electrostatic interactions [29].

In this work, we report on an immobilization strategy for MB probes to enhance their sensitivity when configured in a microarray format. The approach adopted a two pronged strategy: (i) designing appropriate linker structures to minimize probe aggregation effects on the surface and; (ii) the use of a support that provided simple and stable attachment chemistries and minimized electrostatic effects. The MBs contained a C6 amino linker appended to their stems to aid in surface immobilization and also contained discrete polyethylene glycol (dPEG) cross linkers. The dPEG cross linkers are both extremely water/organic soluble and hydrophilic. The commonly used alkyl linker/spacers have the characteristic of being hydrophobic and can suffer from increased aggregation and/or precipitation effects at the surface [30]. The dPEG linkers greatly decrease these artifacts [30;31].

We also used a UV photomodification process as previously described [32;33;34] to activate a poly(methyl methacrylate), PMMA, surface onto which the MBs were attached via carbodiimide coupling chemistry. The same MBs were also attached to glass surfaces using conventional siloxane-based chemistry and the sensitivity of the MBs on glass and PMMA were rigorously compared. The performance of these surface immobilized MBs was also compared to their solution counterpart assays as well. As an example of the performance of this appropriately designed linker and support system for MBs, the loop sequences were used for the analysis of cDNAs generated from *fruitless (fru)* and *Ods-site homeobox (OdsH)* genes extracted from drosophila melanogaster fruitflies. The *fru* gene functions in the central nervous system where it is necessary for sex determination and male courtship behavior while *OdsH* is involved in transcriptional regulation and plays a role in hybrid dysfunctions in spermatogenesis.

Materials and methods

Preparation of cDNA target samples

Three genes, *Odysseus H* (*OdsH*), *fruitless* (*fru*) and a control gene, *Actin5C* (*Act5C*), were chosen for these investigative studies based on their potential influence on the spermatogenesis pathway, role in the sex-determination pathway, and ubiquitous presence in many cell processes. cDNA from these genes was obtained from *Drosophila simulans* due to the species-specific alleles' relevance in an unrelated study. To obtain the sequence of these genes in *D.*

simulans, the sequence of *D. melanogaster* (obtained from FlyBase, http://www.flybase.org) was BLASTed (http://www.ncbi.nlm.nih.gov/BLAST/) against the whole genome sequence of *D. simulans*. Primers were designed to bind to the *D. simulans* sequence, which flanked an intron and did not have any sequence similarity to other genomic DNA. This allowed for a successful amplification of only the sequence of interest and also provided a means of differentiating cDNA amplification from DNA amplification. The PCR primer sequences were as follows:

OdsH-F, CTCATAGTTCCCATCCCCAGAG;

OdsH–R, AGCTATGTAATCGGCCTTCAGAC;

fru–F, ATCCCATCATCTACTTGAAAGATGT;

fru–R, GAGCGGTAGTTCAGATTGTTGTTAT;

Act5C–F, GGATATCCGTAAGGATCTGTATGC;

Act5C–R, CCAAGACAAGCGATCCTTCTTA.

Drosophila simulans stocks were maintained at 20°C, 12-h light:dark cycle. Virgin males were collected, aged 4 days, and then frozen at -80°C between 1-2 hours after “lights on” on the fourth day. RNA was extracted from 35-40 fruit flies using the QIAGEN (Valencia, CA) RNeasy Mini Kit. Reverse transcription was performed using the reverse primer with MMLV Reverse Transcriptase and RNasin from Promega. PCR amplification was performed in a 25-μl volume with 1.5 mM $MgCl_2$, 0.2 mM dNTPs, 1 μM of each primer, 1 unit of *Taq* polymerase, and 5 μl of cDNA template. Samples were amplified through 1 cycle 95°5’, 3 cycles 94°1’/ 56°30”/72°30”, 3 cycles 94°1’/ 53°30”/72°30”, 30 cycles 94°1’/ 50°30”/72°30”. This PCR protocol allows for a single program to work for a variety of primer pairs. The successive reduction of annealing temperatures is referred to as a “touch down” procedure, which is useful when a primer is a good match to the template but has alternative (weaker) binding sites as well. High stringency annealing steps favor binding only to the correct sites, however, at later thermal cycles when the mixture is dominated by PCR products, lower stringency annealing temperatures are less likely to result in binding at alternative sites [35]. The product was run on a 2% agarose gel with both a positive control and a blank (no RNA) negative control, and the appropriate-sized band was extracted and purified using the QIAGEN Gel Extraction Kit. The isolated product was then used as the template for 8 replicate rounds of PCR amplification using the same protocol as stated above, except 1 μl of template was used. The 8 replicates were pooled and purified with the QIAGEN PCR Purification Kit. The final product was then sequenced to confirm that the correct product was obtained, and the sequence was used to design the probe and target.

Design of the MB probe

The oligonucleotide sequences for both the probes and targets are given in Table 1. We designed two different MBs, one for *fru* (MB1) and the other for *OdsH* (MB2) detection. The beacons were labeled at their 5’ ends with a CY 5.5 fluorophore, and at their 3’ ends with BHQ-3 dark quencher. Also, the stem was functionalized with a C6 amino linker (see Figure 1) for attachment to the solid support. The MBs were synthesized by Gene Link Inc. (Hawthorne, NY) and used without further purification.

Immobilization of MBs on solid substrates

PMMA substrates (1 mm thickness) were obtained from Goodfellow (Berwyn, PA) while aldehyde functionalized glass substrates were purchased from Telechem International, Inc. (Sunnyvale, CA). 2-[N-morpholino]ethanesulfonic acid (MES), N-Hydroxysuccinimide (NHS), 1-ethyl-3-(3-dimethylaminopropyl) carbodiimide hydrochloride (EDC), phosphate

and TRIS buffer solutions were obtained from Sigma (Milwaukee, WI). Deionized water (17.9 MΩ) from an E-pure water purification system (Barnstead, Dubuque, IA) was used for preparation of all buffers and rinsing reagents.

MBs were covalently attached onto both PMMA and glass substrates using the appropriate linkage chemistry. For PMMA, the substrates were photoactivated by exposure to broadband UV radiation, which was performed using a UV station equipped with a UV light (500 W DUV, model UXM-501 MA, Ushio America, Cypress, CA). The substrates were placed at a distance of 1 cm from the source for 20 min with a radiation intensity of 15 mW/cm^2. Following UV activation for approximately 30 min, the PMMA substrates were thoroughly rinsed with 2% isopropyl alcohol (IPA), then with ddH_2O followed by drying under nitrogen gas. The PMMA slides were cross-linked with a dPEG spacer (amino dPEG$_{12}$™ acid) obtained from Quanta Biodesign Ltd, (Powell, OH) using carbodiimide coupling chemistry. The surfaces were incubated with 100 mM MES containing 10 mM EDC / 5 mM NHS for 30 min followed by 100 μM of the dPEG for at least 5 h at room temperature after which the slides were thoroughly rinsed in ddH_2O and dried with pressurized air. The amino group of the dPEG$_{12}$ was therefore attached in this step to the PMMA or glass surface leaving the acid functional group of the cross-linker available for attachment of the MB probe, which contained an amino group. Next, the MBs were dissolved in 100 mM MES at pH 5.5 containing 10 mM EDC / 5 mM NHS to a final concentration of 100 nM and spotted onto the substrate by micropipetting 0.2 μl of the appropriate solution onto the solid substrate and incubated for 2 h at room temperature. The spot diameter (obtained by multiplying the number of pixels across the spot by the scanning step resolution) was approximately 2,000 μm. For glass, the aldehyde functionalized slides were incubated with 100 μM dPEG$_{12}$ spacer in phosphate buffer at pH 8.3 for at least 5 h then rinsed thoroughly with ddH_2O and dried with pressurized air. MBs were immobilized to the glass via the dPEG$_{12}$ cross-linker through its carboxy-functional group in a similar fashion as that outlined for PMMA.

Hybridization of MB probes to their targets

For solution-based assays, three different solutions were evaluated: 100 nM MB without target molecules, 100 nM MB with a 10-fold molar excess of non-complementary targets, and 100 nM MB with a 10-fold molar excess of complementary target molecules (see Table 1 for target sequences). All assays were performed in a buffer containing 20 mM TRIS-HCl, 10 mM $MgCl_2$, and 10 mM KCl at pH 7.5. The hybridization reaction was allowed to proceed for 30 min at room temperature, and fluorescence spectra were obtained (λ_{exc} = 675 nm) using a Fluorolog-3 fluorimeter (Jobin Yvon Inc., Edison, NJ). Array-based hybridization was accomplished by incubating the slides containing the immobilized MB probes in a pre-hybridization buffer for 30 min at room temperature, which facilitated the annealing of the stem of the probes. Then, target solutions were placed onto the MB spots and allowed to incubate at room temperature for 2 h followed by fluorescence scanning of the array surface.

Imaging of MB arrays

After hybridization, both glass and PMMA slides were imaged using a home-built near-IR fluorescence scanner, which has been described earlier [34]. In brief, it consisted of a laser diode excitation source lasing at 670 nm with an optical output power of 10 mW (Thorlabs, Newton, NJ). The excitation beam was passed through a neutral density filter (ND 0.6, Thorlabs) and a line filter (670DF20, Omega Optical, Brattleboro, VT). A beam splitter (690DRLP, Omega Optical) was positioned at a 45° angle and focused onto the array surface using a 40X high-numerical aperture (numerical aperture = 0.85) microscope objective (Nikon, Natick, MA). The fluorescence was collected by the same microscope objective and transmitted through the dichroic and finally, through a filter stack consisting of a 700 ALP long-pass filter and a 720 DF20 band-pass filter (Omega Optical). After passing through the filters, the

fluorescence was sent through a pin hole and focused onto a Single Photon Avalanche Diode (SPAD). The entire detector was mounted on an X/Y microtranslational stage interfaced to a computer

Results and Discussion

MB design

Important design parameters associated with MBs are their probe and stem lengths and sequence content because at a given temperature, they largely control the fraction of MBs in the three different conformational states: bound-to-target, stem-loop hairpin or random coil [36]. Generally, the loop sequence consists of 15-25 nucleotide bases, with the sequence content based upon the target sequence and melting temperatures required. The stem typically has 4-6 nucleotide bases and is chosen to have no sequence homology to that of the target. It has been shown that longer stem lengths are accompanied by a lower target affinity and a decreased probe-target hybridization rate, while MBs with short stems have faster hybridization kinetics and improved target affinities but lower sensitivities compared to those with longer stems [37]. On the other hand, MBs with longer loop lengths have improved target affinities and increased kinetic rates, but also display reduced specificities for discrimination between fully matched and mismatched target/loop duplexes [37].

In this study, we designed our MBs with stems containing 5 bases and loops having either 25 nucleotide bases (Figure 1A) or 22 nucleotide bases (Figure 1B). Both MBs had a CY 5.5 fluorophore at their 5’ ends and BHQ-3 (black hole quencher) at their 3’ ends. There are two possible quenching mechanisms that can be envisioned when these probes are in their hairpin configuration: contact quenching or energy transfer. Contact quenching occurs when there is a collision between the fluorophore and quencher, creating a disruption of the energy levels of the excited fluorophore and causing the quencher to dissipate the energy it receives from the fluorophore as heat. Resonance energy transfer (RET) requires spectral overlap between the emission spectrum of the donor (fluorophore) and the acceptor’s (quencher) absorption spectra. We took RET into consideration by selecting the fluorophore and quencher that provided good spectral overlap. For surface immobilization, it was important to have a functional group to aid in the attachment of the MB to the solid support. We also designed our MBs to have a C6 amino linker on the stem. It was also highly desirable to have enough space between the solid support and the probes to enable the probes to be readily accessible to target molecules and also to minimize potential interactions between the MB probes and the surface, which could destabilize the hairpin conformation. We therefore used a $dPEG_{12}$ spacer molecule (see Figure 1C) to keep the probes separated from the surface in order to minimize these artifacts and to avoid any possible steric effects hindering target accessibility to its complementary probe.

Fluorescence of Hybridized MBs in solution

The results shown in Figure 2 indicate that the fluorescence sensitivity (ratio of fluorescence of the probe upon binding to its target with that of the probe in its closed (non-fluorescent) form) of these MBs when hybridized to their complementary DNA targets in solution was 16 for MB1 and 14 for MB2. The MBs incubated without targets or those incubated with non-complementary targets showed minimal amounts of fluorescence.

Immobilization of MBs onto PMMA and glass surfaces

In order to capture complementary targets in an array format, MBs were immobilized onto PMMA and their sensitivities compared to MBs immobilized onto glass supports. For PMMA, the immobilization was done by first activating the surface via exposure to UV irradiation, which introduced a scaffold of carboxylate functional groups on its surface that were then used for coupling to a bifunctional discrete polyethylene glycol cross-linker through carbodiimide

coupling chemistry. This linker molecule consisted of a terminal amine group, which was used to form an amide bond with the surface through the UV-generated carboxylic acids for PMMA or the aldehydes of glass. The PEG_{12} cross-linkers also contained a carboxylic acid group to allow tethering of the MB, which contained an amino group. These linker molecules kept the immobilized MBs spatially removed from the solid surface, improving their hybridization efficiencies [38;39].

Recently, Tan *et al*. reported on the use of poly-T linker molecules to reduce MB associations with the glass surface to which they were attached. They found that when a long poly-T (>25 bases) was used, high negative charges could eventually repel the target DNA and reduce efficiency of duplex formation [15]. The use of the dPEG linkers minimizes this electrostatic artifact because the PEG linker carries no charge at the pH values used for the work reported here.

Another factor we considered when immobilizing the MBs onto the surfaces was the fact that high probe densities typically reduces the binding efficiency of the probes to targets. Vainrub and coworkers have discussed these effects by studying interface electrostatic interactions for chip array hybridizations. In their work, high probe densities lead to high negative charges resulting in strong repulsion between single stranded nucleic acid targets and their surface immobilized probes, giving rise to Coulomb blockage of hybridization [26;27;28]. Also, Peterson and coworkers have described how probe density was a controlling factor for efficient target capture as well as to produce favorable kinetics for target/probe hybridization [29]. They demonstrated that hybridization depends strongly on probe density in both the efficiency of duplex formation and the kinetics of target capture such that with low probe densities, essentially 100% of the surface-immobilized probes were hybridized to their complementary targets with Langmuir-like binding kinetics, while hybridization efficiencies drop to ~10 % in the case of high probe densities. In either case (*i.e.*, low or high probe density), binding saturation at a particular location of the array can lead to limited dynamic range for the expression profiling. To control the immobilization densities, we used low concentrations of probes (100 nM) and limited the immobilization times to less than 2 h. For our PMMA substrates and using carbodiimide attachment chemistry, probe densities were determined to be $\sim 2.4 \times 10^{12}$ molecules/cm^2. These probe densities are comparable to those shown to yield high hybridization efficiencies (2.0×10^{12} molecules/cm^2) [29;40].

Following immobilization of the MBs onto glass or PMMA surfaces, they were incubated in a pre-hybridization buffer containing divalent (Mg^{2+}) cations to facilitate stem annealing to further reduce the background fluorescence of the unhybridized probes. Figures 3A and 3B shows fluorescence images obtained after hybridization with complementary oligonucleotide targets using glass and PMMA supports, respectively. Two different MBs were used in these studies; MB1 and MB2 (see Table 1 for the sequences of these probes). Both images indicated recovery of the fluorescence upon binding with complementary targets. Interestingly, glass exhibited a much higher autoflourescence level at the excitation wavelength used in these studies compared to PMMA. The autofluorescence arises from the substrate itself and is measured in areas on the surface where no MB is found. Figure 4 gives the fluorescence sensitivities of the surface immobilized MBs in comparison to the same probes used in solution. The fluorescence sensitivity found for the PMMA support was ~8 while for glass it was 4 for both MB probes, but both substrates resulted in reduced sensitivities compared to their solution counterparts. In solution, the MBs encounter higher fluorescence sensitivity because they can bind freely with their targets compared to their constrained surface immobilized counterparts. When MBs are in solution with their targets, they can exist in an open conformation (bound to targets) or closed conformation (free of targets). This two-state model is an equilibrium process with the closed state characterized by lower enthalpy than the open state due to base pairing and stacking. The opening rate depends on the unzipping energy of the hairpin probes

[8; 9; 41]. In solution, these hairpin probes diffuse more freely and are unperturbed by surface interactions, hence the ease of interaction with target molecules. On the other hand, surface immobilized probes lack this freedom. In addition, MBs that are immobilized onto solid surfaces have different electrostatic properties at the surface/liquid interface affecting the local ionic strengths and making them differ from those in bulk solution as noted above.

Surface effects can also destabilize the stem structures of the immobilized MB probes, reducing their quenching efficiency when they are in their closed configuration. For the optical set up used in these assays, glass exhibited autofluorescence backgrounds that were 240,000 counts per image pixel while PMMA exhibited a background of 40,000 counts per image pixel. When the autofluorescence background was subtracted from the intensities of the MBs probes without targets (closed configuration) or that of these MBs after incubation with non-complementary targets, the net signal was 40,000 for both surfaces. The lack of difference between these values indicates that both surfaces affect the closed configurations of the surface-immobilized MBs to the same degree, which is not too surprising given the fact that in both PMMA and glass, a monolayer of the dPEG-linker is formed over the underlying surfaces. However, upon binding of the MB probes to their full complementary targets, glass exhibited intensities of 160,000 counts per image pixel while PMMA showed a value of 340,000 counts per image pixel (both were background subtracted). The lower MB sensitivity on glass surfaces could arise due to static charging. On the other hand, PMMA exhibited better fluorescence sensitivity due to its electrostatic surface effects (thermodynamic equilibrium distribution), which affects the probe-target binding strength near the surface in a more favorable manner. It has been shown that strong attraction of a probe-target duplex for the surface promotes duplex formation, while surface repulsion of the probe-target duplex will shift the hybridization equilibrium toward melting of the duplexes [27].

Analytical sensitivity of MBs immobilized onto PMMA substrates

When carrying out MB hybridization assays, it is desirable for the loop sequence to only hybridize to the specific sequence of interest and also to work within useful target concentrations. We immobilized MB probes onto PMMA surfaces with the loop sequences corresponding to the *OdsH* gene (MB1) and *fru* gene (MB2) of *Drosophila melanogaster*. The target samples were prepared by creating cDNA from messenger RNA (mRNA) through reverse transcription. Before being used in the hybridization assays, the cDNAs were denatured for 5 min at 95°C and then immediately cooled on ice. Figure 5 shows the fluorescence images obtained after hybridization of MB probes immobilized onto PMMA surfaces without targets (A), upon hybridization with complementary cDNAs (B) and after hybridization with non-complementary cDNAs (C). *Actin 5C (Act5C)* gene is non-complementary to both MB1 and MB2 and therefore was used as a negative control in these studies (see Table 1).

For both immobilized probes, those without targets (A) and with non-complementary targets (C) did not show any significant fluorescence, while those with perfect complementary targets (B) exhibited strong fluorescence. The MB probes did bind to their target sequences forming probe-target hybrids that were more stable than the stem hybrid. Only perfect complementary hybrids were sufficiently stable to force the stem-hybrid to open, resulting in higher fluorescence.

The analytical sensitivity for reporting on the concentration of the solution complements using these immobilized MB probes was then determined using different concentrations of the targets and constructing calibration plots. For each MB probe, the experiments were performed in triplicate on different PMMA slides using a solution cDNA concentration ranging from 100 nM to 2.5 μM. Figure 6 shows the calibration plots for the observed fluorescence intensities versus target concentrations for MB1 (Figure 6A) and MB2 (Figure 6B). Low target concentrations required longer reaction times to reach steady-state while increased target

concentrations promoted more intermolecular duplex formation. The plots were linear with a correlation coefficient of $R^2 = 0.96$ for MB1 and $R^2 = 0.97$ MB2.

The presence and abundance of targets within a sample are usually indicated by the intensity of the hybridization signal at the corresponding probe sites. Alternatively, the abundance of the targets can be obtained by reverse transcription (RT)-PCR based assays, which are common methods for comparing mRNA levels in different sample populations. The mRNA levels are measured and normalized to reference genes, which allow each gene expression to be measured as a numerical value that enables direct comparison between experiments. The relative abundance of the genes used in this study has been determined and the normalized expression values obtained were *Fru* mRNA (9.12), *OdsH* mRNA (3.43) and *Actin 5 C* mRNA (11.24) [42]. These results indicate that the *Fru* mRNA is highly abundant in D. Simulans, while the *OdsH* is near the threshold of detection of conventional arrays.

Conclusion

These studies were based on the concept that proper MB design, careful solid support choice with robust surface chemistries could lead to improved sensitivities of surface immobilized MBs. We chose a surface modification procedure described earlier in our lab [34] to produce functional scaffolds consisting of carboxylic acid groups that allowed for the covalent attachment of amine-functionalized MB probes onto PMMA surfaces through carbodiimide coupling. These processes involved only broadband UV exposure of the polymer surface followed by carbodiimide coupling of amine-containing MB probes to the surface (via an amide bond). Surface-bound probes require enough interstitial space to improve hybridization efficiency. Therefore, we employed dPEG cross-linker molecules to minimize any steric effects that might occur as well as minimizing surface aggregation effects. MBs immobilized onto PMMA showed higher fluorescence restoration compared to those immobilized on glass surfaces. In this study, PMMA was found to be a better substrate compared to glass for the designed probes and wavelengths used for their interrogation. The ability to perform quantitative assays using these type of MB probes and proper substrates will be a useful tool in gene expression analysis.

Acknowledgments

The authors would like to thank the National institutes of Health (National Institute of Biomedical Imaging and Bioengineering, R24-EB002115), the National Science Foundation under Grant Number EPS-0346411 and the State of Louisiana Board of Regents for financial support of this work.

References

1. Tyagi S, Kramer FR. Molecular beacons: probes that fluoresce upon hybridization. Nat Biotechnol 1996;14:303–308. [PubMed: 9630890]
2. Vet JAM, Majithia AR, Marras SAE, Tyagi S, Dube S, Poiesz BJ, Kramer FR. Multiplex detection of four pathogenic retroviruses using molecular beacons. Proc Natl Acad Sci USA 1999;96:6394–6399. [PubMed: 10339598]
3. Tyagi S, Bratu DP, Kramer FR. Multicolor molecular beacons for allele discrimination. Nat Biotechnol 1998;16:49–53. [PubMed: 9447593]
4. Kostrikis LG, Tyagi S, Mhlanga MM, Ho DD, Kramer FR. Spectral genotyping of human alleles. Science 1998;279:1228–1229. [PubMed: 9508692]
5. Tang Z, Wang K, Tan W, Li J, Liu L, Guo Q, Meng X, Ma C, Huang S. Real-time monitoring of nucleic acid ligation in homogeneous solutions using molecular beacons. Nucleic Acids Res 2003;31:e148/1–e148/7. [PubMed: 14627838]
6. Mhlanga, MM.; Malmberg, L. Methods (San Diego, CA, United States). Vol. 25. 2001. Using Molecular Beacons to Detect Single-Nucleotide Polymorphisms with Real-Time PCR; p. 463-471.

7. Situma C, Hashimoto M, Soper SA. Merging microfluidics with microarray-based bioassays. Biomol Eng 2006;23:213–231. [PubMed: 16905357]
8. Bonnet G, Tyagi S, Libchaber A, Kramer FR. Thermodynamic basis of the enhanced specificity of structured DNA probes. Proc Natl Acad Sci USA 1999;96:6171–6176. [PubMed: 10339560]
9. Bonnet G, Krichevsky O, Libchaber A. Kinetics of conformational fluctuations in DNA hairpin-loops. Proc Natl Acad Sci USA 1998;95:8602–8606. [PubMed: 9671724]
10. Fang X, Liu X, Schuster S, Tan W. Designing a novel molecular beacon for surface-immobilized DNA hybridization studies. J Am Chem Soc 1999;121:2921–2922.
11. Liu X, Farmerie W, Schuster S, Tan W. Molecular beacons for DNA biosensors with micrometer to submicrometer dimensions. Anal Biochem 2000;283:56–63. [PubMed: 10929808]
12. Steemers FJ, Ferguson JA, Walt DR. Screening unlabeled DNA targets with randomly ordered fiber-optic gene arrays. Nat Biotechnol 2000;18:91–94. [PubMed: 10625399]
13. Epstein JR, Leung APK, Lee K-H, Walt DR. High-density, microsphere-based fiber optic DNA microarrays. Biosens & Bioelectron 2003;18:541–546.
14. Brown LJ, Brown T, Cummins J, Hamilton A. Molecular beacons attached to glass beads fluoresce upon hybridization to target DNA. Chem Commun 2000:621–622.
15. Yao G, Tan W. Molecular-beacon-based array for sensitive DNA analysis. Anal Biochem 2004;331:216–223. [PubMed: 15265725]
16. Li J, Tan W, Wang K, Xiao D, Yang X, He X, Tang Z. Ultrasensitive optical DNA biosensor based on surface immobilization of molecular beacon by a bridge structure. Anal Sci 2001;17:1149–1153. [PubMed: 11990586]
17. Culha M, Stokes DL, Griffin GD, Vo-Dinh T. Application of a miniature biochip using the molecular beacon probe in breast cancer gene BRCA1 detection. Biosens & Bioelectron 2004;19:1007–1012.
18. Wang H, Li J, Liu H, Liu Q, Mei Q, Wang Y, Zhu J, He N, Lu Z. Label-free hybridization detection of a single nucleotide mismatch by immobilization of molecular beacons on an agarose film. Nucleic Acids Res 2002;30:e61/1–e61/9. [PubMed: 12060699]
19. Du H, Disney MD, Miller BL, Krauss TD. Hybridization-Based Unquenching of DNA Hairpins on Au Surfaces: Prototypical \“Molecular Beacon\” Biosensors. J Am Chem Soc 2003;125:4012–4013. [PubMed: 12670198]
20. Du H, Strohsahl Christopher M, Camera J, Miller Benjamin L, Krauss Todd D. Sensitivity and specificity of metal surface-immobilized “molecular beacon” biosensors. J Am Chem Soc 2005;127:7932–7940. [PubMed: 15913384]
21. Swearingen CB, Wernette DP, Cropek DM, Lu Y, Sweedler JV, Bohn PW. Immobilization of a Catalytic DNA Molecular Beacon on Au for Pb(II) Detection. Anal Chem 2005;77:442–448. [PubMed: 15649039]
22. Fan C, Plaxco KW, Heeger AJ. Electrochemical interrogation of conformational changes as a reagentless method for the sequence-specific detection of DNA. Proc Natl Acad Sci USA 2003;100:9134–9137. [PubMed: 12867594]
23. Sauthier ML, Carroll RL, Gorman CB, Franzen S. Nanoparticle Layers Assembled through DNA Hybridization: Characterization and Optimization. Langmuir 2002;18:1825–1830.
24. Jin R, Wu G, Li Z, Mirkin CA, Schatz GC. What controls the melting properties of DNA-linked gold nanoparticle assemblies? J Am Chem Soc 2003;125:1643–1654. [PubMed: 12568626]
25. Zuo X, Yang X, Wang K, Tan W, Li H, Zhou L, Wen J, Zhang H. Improving the performance of immobilized molecular beacons through cleavage. Anal Chim Acta 2006;567:173–178.
26. Vainrub A, Pettitt BM. Thermodynamics of association to a molecule immobilized in an electric double layer. Chem phys Lett 2000;323:160–166.
27. Vainrub A, Pettitt BM. Surface electrostatic effects in oligonucleotide microarrays: Control and optimization of binding thermodynamics. Biopolymers 2003;68:265–270. [PubMed: 12548628]
28. Vainrub A, Pettitt BM. Theoretical aspects of genomic variation screening using DNA microarrays. Biopolymers 2004;73:614–620. [PubMed: 15048785]
29. Peterson AW, Heaton RJ, Georgiadis RM. The effect of surface probe density on DNA hybridization. Nucleic Acids Res 2001;29:5163–5168. [PubMed: 11812850]

30. Davis, PD.; Crapps, EC. Application: WO. 2004. A method for selective and specific preparations of discrete polyethylene glycol compounds, (Quanta Biodesign, Ltd., USA); p. 108

31. Kidambi S, Chan C, Lee I. Selective Depositions on Polyelectrolyte Multilayers: Self-Assembled Monolayers of m-dPEG Acid as Molecular Template. J Am Chem Soc 2004;126:4697–4703. [PubMed: 15070388]

32. Wei S, Vaidya B, Patel AB, Soper SA, McCarley RL. Photochemically Patterned Poly(methyl methacrylate) Surfaces Used in the Fabrication of Microanalytical Devices. J Phys Chem B 2005;109:16988–16996. [PubMed: 16853163]

33. McCarley RL, Vaidya B, Wei S, Smith AF, Patel AB, Feng J, Murphy MC, Soper SA. Resist-Free Patterning of Surface Architectures in Polymer-Based Microanalytical Devices. J Am Chem Soc 2005;127:842–843. [PubMed: 15656615]

34. Situma C, Wang Y, Hupert M, Barany F, McCarley RL, Soper SA. Fabrication of DNA microarrays onto poly(methyl methacrylate) with ultraviolet patterning and microfluidics for the detection of low-abundant point mutations. Anal Biochem 2005;340:123–135. [PubMed: 15802138]

35. Meyer, A. Molecular Systematics. 2. Hillis, David M., editor. 1996.

36. Tsourkas A, Behlke MA, Bao G. Structure-function relationships of shared-stem and conventional molecular beacons. Nucleic Acids Res 2002;30:4208–4215. [PubMed: 12364599]

37. Tsourkas, Bao G. Shedding light on health and disease using molecular beacons. Briefings in Functional Genomics & Proteomics 2003;1:372–384. [PubMed: 15239884]

38. Lin Z, Strother T, Cai W, Cao X, Smith LM, Hamers RJ. DNA attachment and hybridization at the silicon (100) surface. Langmuir 2002;18:788–796.

39. Pena SRN, Raina S, Goodrich GP, Fedoroff NV, Keating CD. Hybridization and Enzymatic Extension of Au Nanoparticle-Bound Oligonucleotides. J Am Chem Soc 2002;124:7314–7323. [PubMed: 12071740]

40. Vainrub A, Pettitt BM. Sensitive Quantitative Nucleic Acid Detection Using Oligonucleotide Microarrays. J Am Chem Soc 2003;125:7798–7799. [PubMed: 12822987]

41. Grunwell JR, Glass JL, Lacoste TD, Deniz AA, Chemla DS, Schultz PG. Monitoring the Conformational Fluctuations of DNA Hairpins Using Single-Pair Fluorescence Resonance Energy Transfer. J Am Chem Soc 2001;123:4295–4303. [PubMed: 11457196]

42. N, aMAF.; Moehring, AJ.; Teeter, JC. Genome-wide patterns of expression in drosophila pure species and hybrid males.11 Examination of multiple species hybridizations,platforms, and life-cycle stages. Mol Biol Evol. 2006 in press.

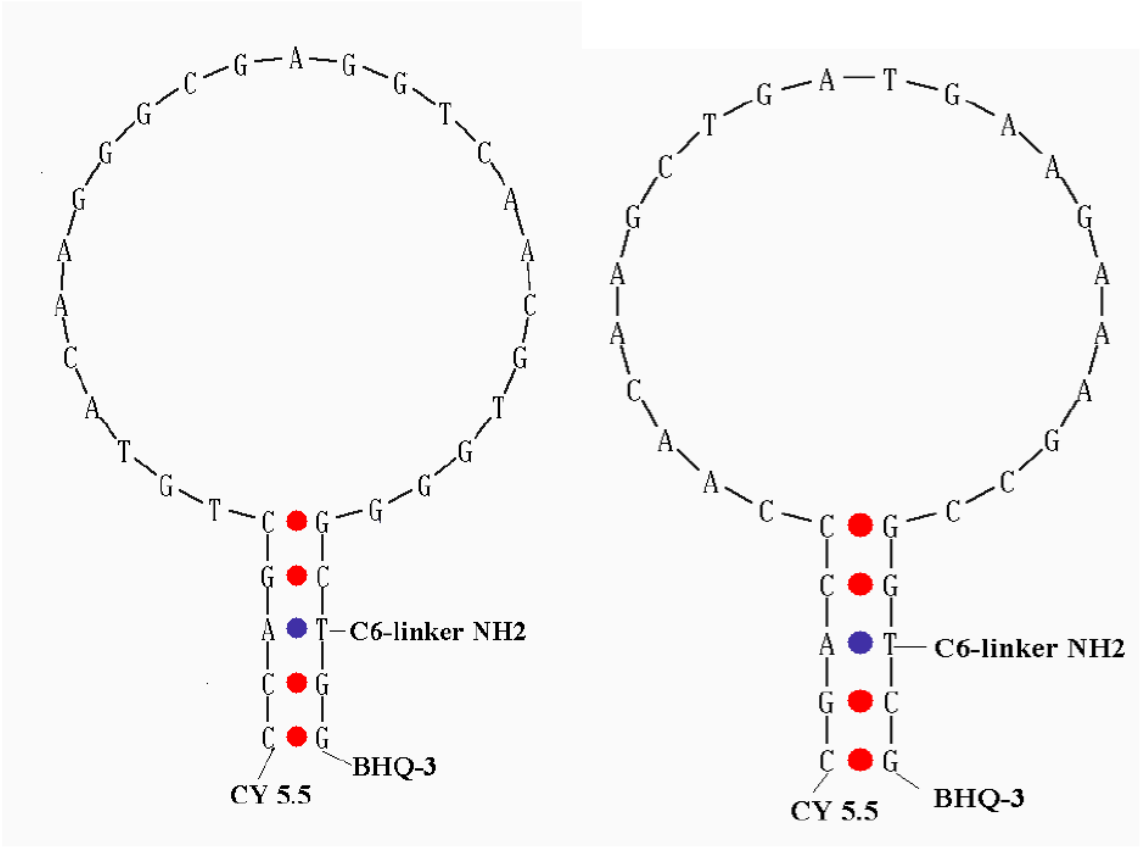

Figure 1.

The structure of molecular beacon probes used for the detection of *fru* gene MB1 (a) and ods-H gene MB2 (b). Their stem structures possessed a C6 amino linker to aid in surface immobilization using a discrete polyethylene glycol (dPEG) cross-linker (c).

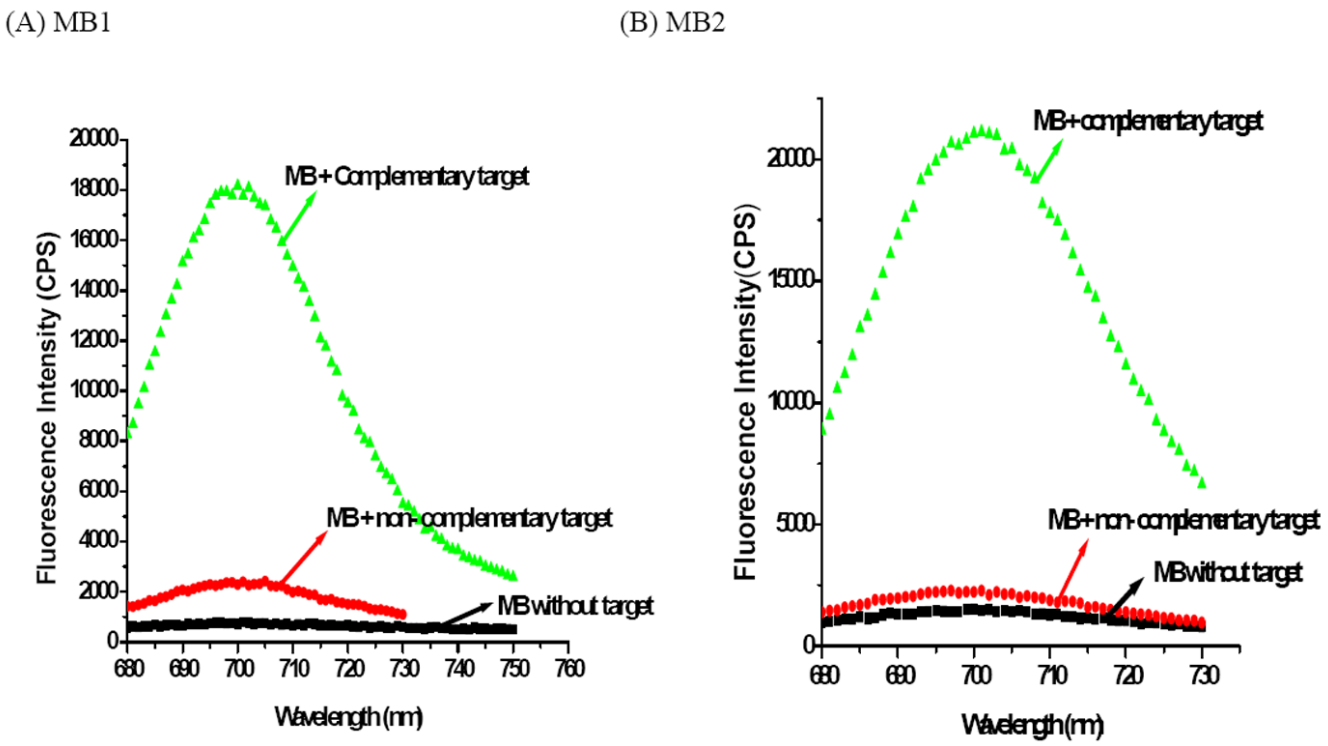

Figure 2.

Solution-based hybridization results for MB1 (A) and MB2 (B), respectively. Three solutions were used; 100nM MB without target molecules, 100 nM MB with a 10-fold molar excess of non-complementary target and 100 nM MB with a 10-fold molar excess of complementary target molecules. The solutions were incubated for 30 min in a hybridization buffer consisting of 20 mM Tris-HCl, 10 mM $MgCl_2$, and 10 mM KCl at pH 7.5. The fluorescence spectra were obtained using λ_{exc} = 675 nm.

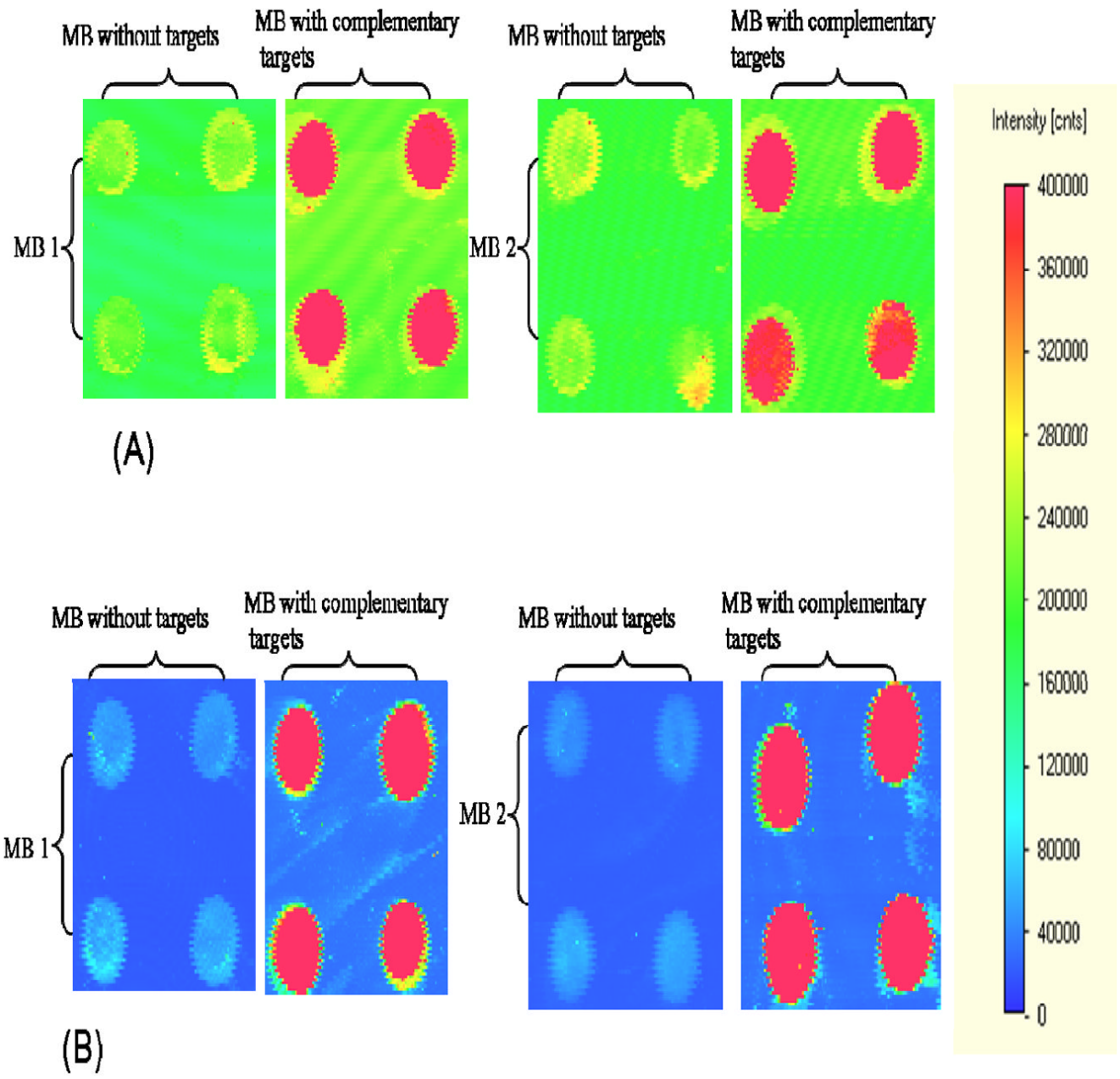

Figure 3.

Comparison of the fluorescence hybridization results for molecular beacons immobilized onto glass (A) and poly(methyl methacrylate), PMMA, (B). Functionalized PMMA and glass substrates were used for coupling a bifunctional dPEG cross-linker through carbodiimide coupling chemistry. The solution complements were synthetic oligonucleotides (see underlined sequences for T1 and T2 in Table 1) set at a concentration of 100 nM, which were allowed to hybridized with the array in a humidified chamber for 2 h prior to fluorescence scanning. Fluorescence images were obtained before hybridization (left) and after hybridization to the immobilized MB probes with their fully complementary targets (right) for both MB1 and MB2.

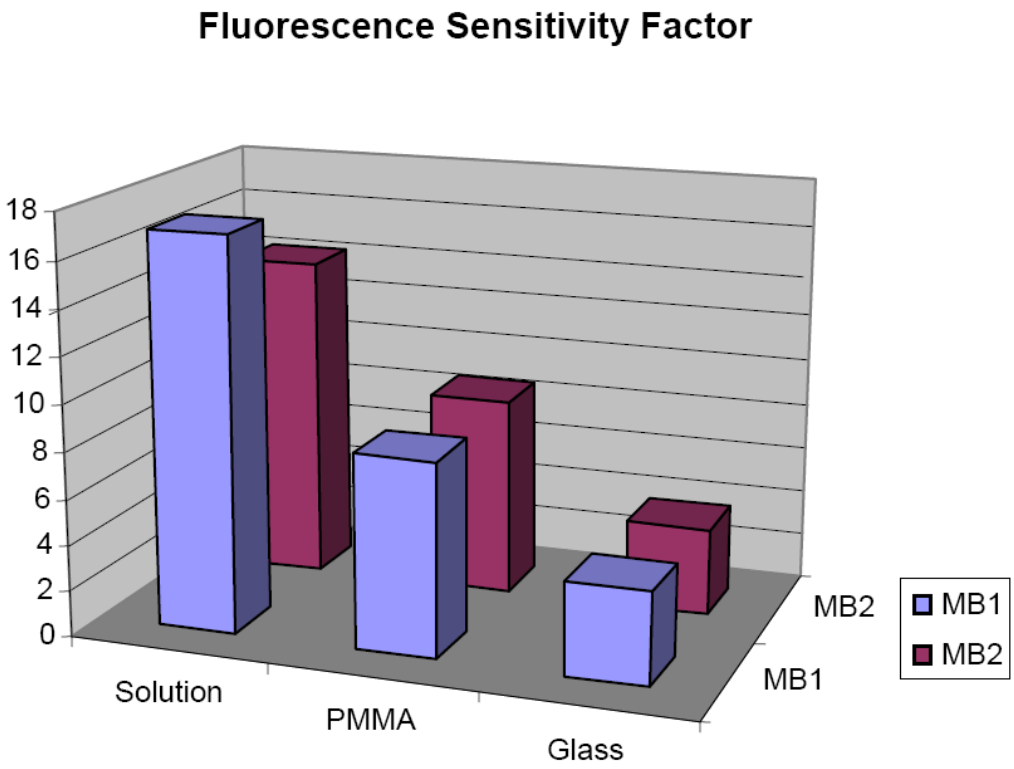

Figure 4.
Fluorescence sensitivity ratios for solution-based hybridization events and surface-immobilized MBs using glass and PMMA substrates.

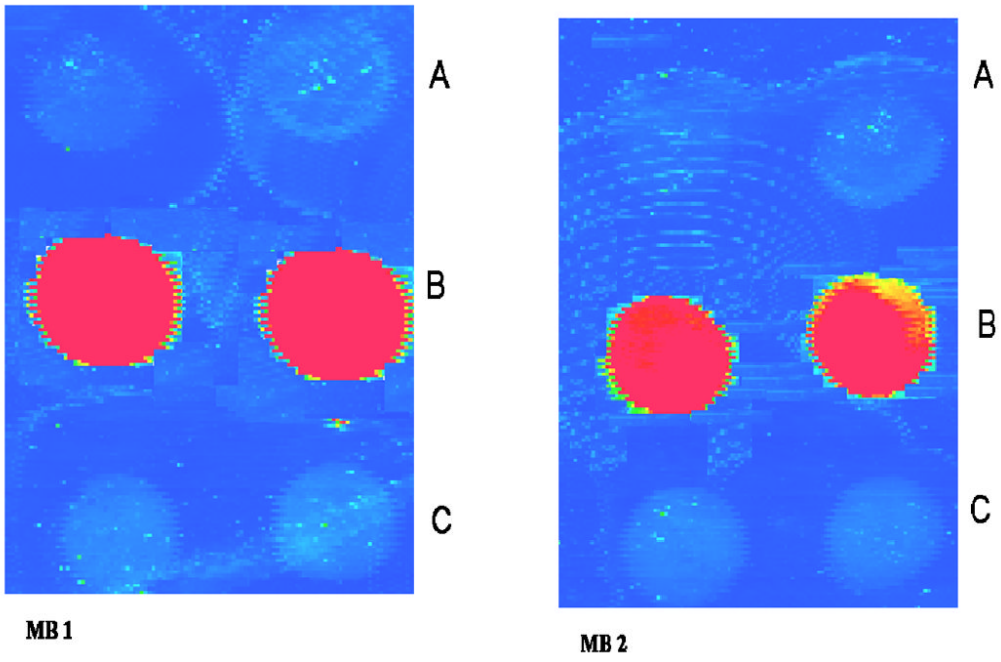

Figure 5.

Analysis of cDNAs generated from drosophila melanogaster fruit flies for the *fruitless* (*fru*) and *Ods-site homeobox* (*OdsH*) genes. Array measurements were performed using the MB probes immobilized onto PMMA substrates. PMMA substrates were activated by exposure to UV radiation followed by reaction with the dPEG cross-linker and finally, immobilization of the MB probes to the dPEG surface using a 100 nM solution. These probes were then used for hybridization with complementary and non-complementary targets for 2 h at room temperature. Fluorescence images were obtained after hybridization of surface immobilized molecular beacons; (A) without targets, (B) with fully complementary targets (C) with non-complementary targets. The complementary targets T1 / T2 and non-complementary targets T3 (refer to Table 1 for their sequences) are cDNAS extracted from drosophila melanogaster fruit flies.

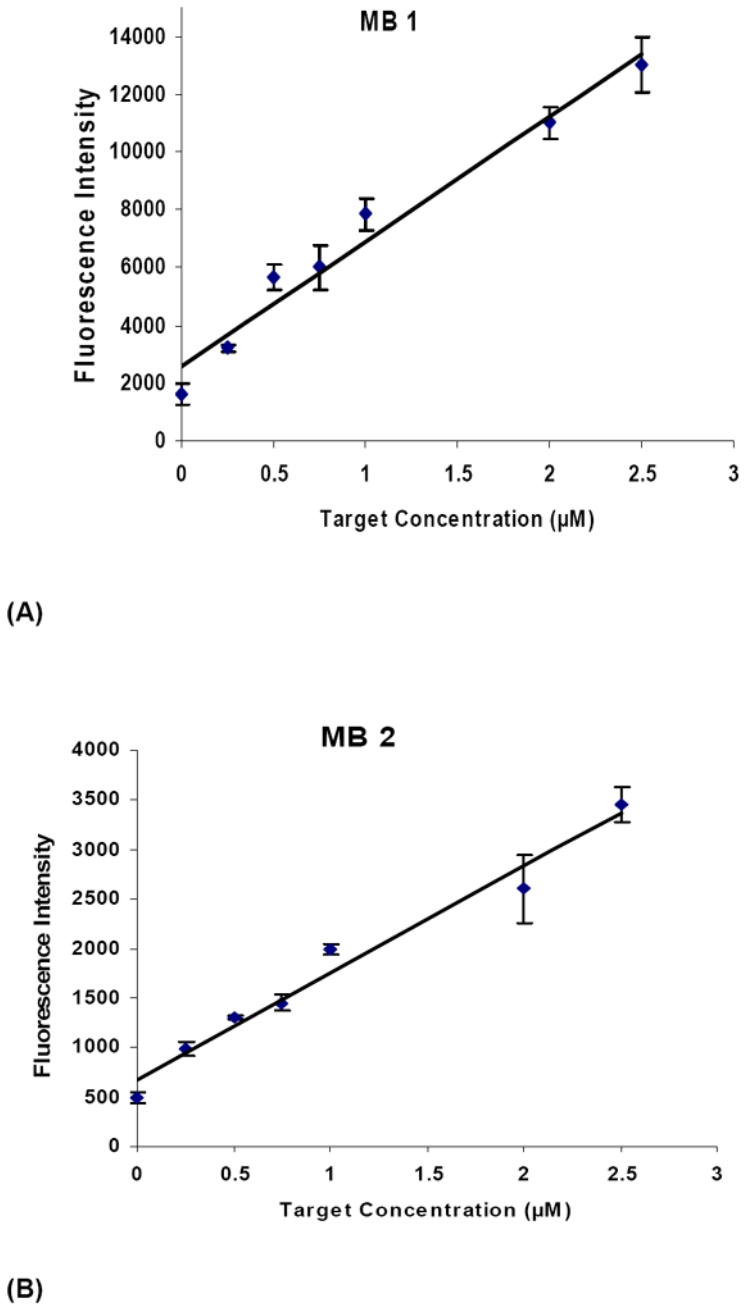

Figure 6.

The calibration plots for the surface fluorescence measurements versus target concentrations for MB1 (A) and MB2 (B), respectively. The MB probes were immobilized onto PMMA slides and used for binding with their complementary targets with concentrations ranging from 100 nM to 2.5 μM. The error bars represent the standard deviation for three measurements.

Table 1
Molecular beacon probes and target sequences

MB1 and MB2 represent the molecular beacon used for these studies and their respective sequences. Lower case letters denote the stem sequences of the beacons while the upper case letters are the recognition loop sequences. T1 and T2 are target sequences complementary to MB1 and MB2, respectively. The underlined sequence is the section of the target complementary to the MBs. T3 is a non-complementary sequence to both MB1 and MB2. All targets (T1, T2, and T3) were cDNAs extracted from *Drosophila melanongaster* for *fruitless* (*fru*), *Ods-site homeobox* (*OdsH*) and *Actin 5C (Act5C)* genes, respectively. Actin is non-complementary both to MB 1 and MB 2 and it was used as a negative control in these studies.

	Sequence 5' to 3'
MB1	(CY5.5) - ccagcTGTACAAGGGCGAGGTCAACGTGGG gctgg-(BHQ-3)
MB2	(CY5.5) –cgaccCAACAAGCTGATGAAGAAAGCCggtcg-(BHQ-3)
T1	GCAGCGAACTCTGA<u>CCCACGTTGACCTCGCCCTTGTAC</u>ATGAAGTCGAGCAGAGATCGCATCTCT GAGTATCTGACATCTTTCAAGTAGATGATGGGATA
T2	CTTCTTCGCCTGCCGTTCGAT<u>GGCTTTCTTCATCAGCTTGTTG</u>CGCTGGGCTAGTTCT TTGGCGCGAAAGTTCGCTAAGTGGAATGGGGTTACCACTGCAGCTCTGGGGATGGGA ACTATGAAAA
T3	TGCACAATGGAGGGGCCGGNACTCGTCNTACTCCTGCTTGGAGATCCACATCTGCTGG AAGGTGGACAGCGAAGCCAGGATGGAACCACCNATCCAGACAGAGTACTTGCGCTCT GGTGGGGCAATGATCTTGATCTTCATGGTCNACGGGGCCAGGGCGGTGATCTCCTTCT GCATACNGTCGGCGATGCCAGGGTACATGGTGGTGCCACCNGACAGCACGGTGTTGGC ATACANATCCTTACGGATATCCAAGC